Fluid flow increases mineralized matrix deposition in 3D perfusion culture of marrow stromal osteoblasts in a dose-dependent manner

Gregory N. Bancroft*†, Vassilios I. Sikavitsas*†‡, Juliette van den Dolder§, Tiffany L. Sheffield¶, Catherine G. Ambrose¶, John A. Jansen§, and Antonios G. Mikos*‖

*Department of Bioengineering, Rice University, 6100 Main, Houston, TX 77005; §Department of Biomaterials, College of Dental Science, University Medical Center Nijmegen, P.O. Box 9101, 6500 HB Nijmegen, The Netherlands; and ¶Department of Orthopaedics, University of Texas, 6431 Fannin Suite 6148, Houston, TX 77030

Edited by Robert Langer, Massachusetts Institute of Technology, Cambridge, MA, and approved August 6, 2002 (received for review May 16, 2002)

Bone is a complex highly structured mechanically active 3D tissue composed of cellular and matrix elements. The true biological environment of a bone cell is thus derived from a dynamic interaction between responsively active cells experiencing mechanical forces and a continuously changing 3D matrix architecture. To investigate this phenomenon *in vitro*, marrow stromal osteoblasts were cultured on 3D scaffolds under flow perfusion with different rates of flow for an extended period to permit osteoblast differentiation and significant matrix production and mineralization. With all flow conditions, mineralized matrix production was dramatically increased over statically cultured constructs with the total calcium content of the cultured scaffolds increasing with increasing flow rate. Flow perfusion induced *de novo* tissue modeling with the formation of pore-like structures in the scaffolds and enhanced the distribution of cells and matrix throughout the scaffolds. These results represent reporting of the long-term effects of fluid flow on primary differentiating osteoblasts and indicate that fluid flow has far-reaching effects on osteoblast differentiation and phenotypic expression *in vitro*. Flow perfusion culture permits the generation and study of a 3D, actively modeled, mineralized matrix and can therefore be a valuable tool for both bone biology and tissue engineering.

Bone is a complex, highly organized tissue consisting of a structured extracellular matrix composed of inorganic and organic elements containing a conglomeration of cell types responsible for its metabolism and upkeep that are responsive to a variety of signals (1). As would be expected from the skeleton's central role in support and structural integrity, bone cells cultured *in vitro* respond to a variety of different mechanical signals including fluid flow, hydrostatic pressure, and substrate deformation.

Current studies indicate that fluid flow is a potentially stronger stimulus for bone cell behavior than either hydrostatic compression (2) or substrate deformation (3, 4). The *in vitro* mechanical stimulation of bone cells by fluid flow has been reported to impact the levels of many biochemical factors including intracellular calcium (5, 6), nitric oxide (4, 7–9), prostaglandin E_2 (3, 4, 7, 8), the expression of the genes for osteopontin, cyclooxygenase-2, and c-Fos (6, 10–12) as well as other intracellular messengers and transcription factors (6, 13–15). This mechanostimulation of bone cells *in vitro* by fluid flow mimics the physiological response of bone cells *in vivo* where pressure gradients from mechanical loading of locomotion and other stressors deform the mineralized bone matrix and move extracellular fluid radially outward toward the cortex through the lacunocanalicular network (16–19). Mechanical loading of bone plays an important role because it can both increase bone formation and decrease bone resorption (1). Indeed, its absence can lead to lower bone matrix protein production, mineral content, and bone formation plus increased bone resorption (1).

Various mechanisms have been suggested for the manner in which bone cells are stimulated by fluid flow including streaming potentials (20, 21), wall shear stress (13), and chemotransport (22). Recent study (7) suggests that flow-derived shear stress is the most significant and primary mediator of fluid flow mechanical stimulation at least as far as its impact on the chemical mediators nitric oxide and prostaglandin E_2.

In these previous studies, cells were exposed to flow in a 2D environment. However, bone is an anisotropic tissue that experiences mechanical stress and shapes itself in response to such stress in a 3D manner (1). Flow perfusion culture of cells seeded into a 3D scaffold can both potentially provide fluid flow-induced mechanical stimulation and permit true multilayered 3D cellular growth and organization (23, 24). This attempted *in vivo* replication of the organization and growth of cells in 3D structures has been shown to enhance the phenotypic expression of bone cells cultured in such a manner (23, 24).

Particularly noteworthy for applications in the field of tissue engineering are recent studies suggesting that the organization of bone cells into 3D structures is crucial for *ex vivo* tissue formation (25) and that the phenotypic behavior of cultured cells can depend greatly on this 3D matrix structure and organization (26). This is especially important for bone cells exposed to long-term flow forces as bone cells exposed to mechanical strain increase their own bone matrix production (27). Additionally, studies have shown that exposing bone cells to mechanical forces induces changes in both the organization of the internal cellular cytoskeleton (11) and also the contact points at which the cytoskeleton interacts with the mineralized bone extracellular matrix (28). The true biological environment of a bone cell is thus derived from a dynamic interaction between responsively active cells experiencing mechanical forces and a continuously changing 3D matrix architecture.

Such interactions are quite consequential during osteoblast differentiation and bone development, which integrate the action of several signals including cytokines/growth factors, extracellular matrix molecules, and cell–cell interactions (29). Investigation into the *ex vivo* behavior and differentiation of osteoblasts from preliminary precursor cells to mineralizing, matrix-producing osteoblasts would thus benefit from a culture environment that emulates the 3D mechanically active milieu of *in vivo* bone tissue. Based on the above discussion, such a culture environment would be expected to impact the growth and differentiation of the cultured bone cells as well as enhance the investigation into aspects of osteoblast behavior such as mineralized matrix production and extracellular matrix organization. Although most studies of bone cells exposed to fluid flow have been conducted by using planar culture surfaces for relatively short periods of time (hours), analysis into *ex vivo* bone

This paper was submitted directly (Track II) to the PNAS office.

Abbreviations: SEM, scanning electron microscopy; AP, alkaline phosphatase.

†G.N.B. and V.I.S. contributed equally to this work.

‡Present address: Department of Chemical Engineering and Materials Science, University of Oklahoma, 100 East Boyd, Norman, OK 73019.

‖To whom reprint requests should be addressed at: Department of Bioengineering, Rice University, P.O. Box 1892, MS-142, Houston, TX 77251-1892. E-mail: mikos@rice.edu.

www.pnas.org/cgi/doi/10.1073/pnas.202296599

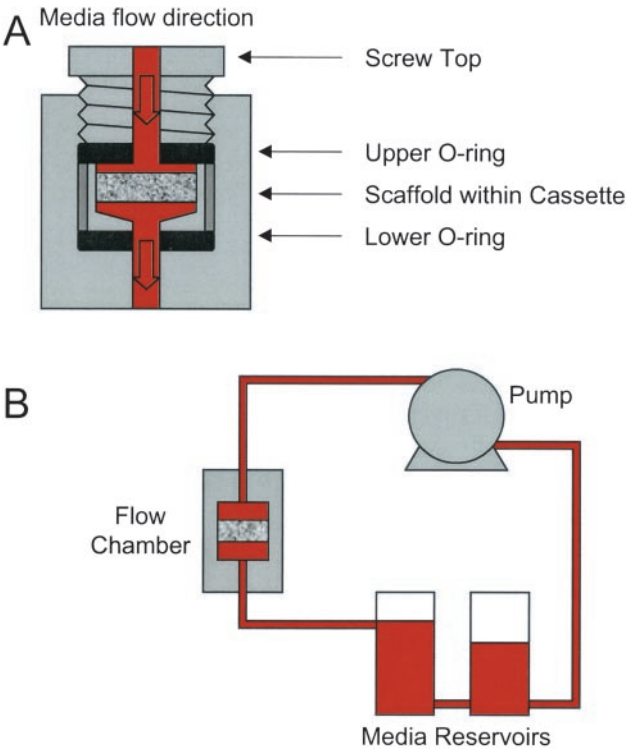

Fig. 1. Schematic of flow perfusion system. (*A*) Design of an individual flow chamber. (*B*) Relation to the flow perfusion circuit.

tissue production and osteoblast matrix generation and organization requires longer culture periods (days to weeks) to allow for the evolution of a mineralized bone matrix.

In this study we examined the effects of flow perfusion culture on the 3D culture of differentiating marrow stromal osteoblasts seeded on a 3D scaffold. We investigated the effects of prolonged flow perfusion culture on the biochemical behavior and extracellular matrix development of differentiating primary bone cells grown in a 3D environment exposed to varying rates of fluid flow.

Materials and Methods

Isolation of Rat Marrow Stromal Cells and Culture of Marrow Stromal Osteoblasts. Rat marrow stromal cells were isolated by using established methods as described (30). Cells were cultured for 6 d in α-MEM (Life Technologies, Grand Island, NY) supplemented with 10% FBS, standard cell culture antibiotics, and the osteogenic media supplements dexamethasone (10^{-8} M), ascorbic acid (50 μg/ml), and β-glycerophosphate (10 mM) (all from Sigma). On day 6, cells were trypsinized and counted in for seeding on the titanium mesh scaffolds.

Titanium Fiber Mesh Scaffolds and Cell Seeding. Titanium fiber mesh scaffolds were prepared by die-punching discs from a sheet of sintered nonwoven titanium fiber mesh (Bekaert, Zwevegem, Belgium). Scaffolds had a volumetric porosity of 86% and a fiber diameter of 40 μm. The average pore size of the mesh was $\approx$250 μm. As used, the scaffolds were disk-shaped with a diameter of 10 mm, a thickness of 0.8 mm, and a weight of $\approx$40 mg.

Before use, the scaffolds were sterilized by autoclave and each was press-fitted into a flow system cassette (Fig. 1*A*). Subsequently, the titanium meshes were placed in a 6-well plate, and a cell suspension of 5×10^5 cells in 300 μl was added to the top of each scaffold. Scaffolds for both flow perfusion culture and static culture were seeded by using cassettes to ensure a similar seeding for each culture method. Seeded titanium meshes in the cassettes were placed into standard 6-well plates, and after 2 h sufficient media were added to each well to cover the scaffolds. Cells were allowed to attach overnight, and thereafter the meshes were used in the flow perfusion system.

Flow Perfusion Culture. A flow perfusion culture system was developed. It consisted of six flow chambers custom-machined in a block of polymethylmethacrylate (commonly referred to as "Plexiglas"). Each flow chamber contained a cassette sealed by two neoprene o-rings held in place by a screw-top (Fig. 1). Each flow chamber contained a titanium mesh scaffold. Media flowed top to bottom through the scaffold to prevent the trapping of air bubbles beneath the scaffold, which could alter the flow pattern on the surface of the scaffold. The press-fitting of the scaffold into each cassette as well as the o-ring sealing ensured that the only flow path was through the scaffold. Flow through each chamber was driven by a multichannel roller pump (Cole–Parmer) with each flow chamber on its own independent pumping circuit to ensure a consistent, controllable flow rate to each flow chamber. All flow chambers drew media from a common reservoir. In the complete flow perfusion culture circuit (Fig. 1*B*), media was drawn from the first media reservoir, pumped through each flow chamber, and returned to a second reservoir, which was connected to the first reservoir. The fluid head pressure then returned the media to the first reservoir where the flow cycle repeated. This two-reservoir design allowed essentially a complete change of the media by simply closing the connection between the two reservoirs, emptying both reservoirs, filling the first reservoir with fresh media, and pumping the old media into the second reservoir where it was removed before reestablishing the connection between the two reservoirs. The entire flow circuit was connected with platinum-cured silicon tubing (Cole–Parmer), which has a high permeability to both carbon dioxide and oxygen thereby ensuring adequate gas equilibration with the surrounding incubator air. Before use, the polymethylmethacrylate components (flow chamber block, cassettes, and screw-tops) were sterilized by ethylene oxide gas, whereas the remaining components (tubing, reservoirs, and connectors) were sterilized by autoclave.

For these experiments, the flow perfusion culture system was assembled by using appropriate sterile techniques in a laminar flow hood and filled with $\approx$200 ml of media. The cassettes with the seeded scaffolds were sealed in the individual flow chambers and the systems placed into standard cell culture incubators with an environment of 37°C and 5% CO_2. Scaffolds were cultured at low, medium, and high media flow rates of 0.3, 1, and 3 ml/min, respectively, for a total of 16 d. The flow rate was initially set at 0.3 ml/min for all systems and subsequently increased to 1 and 3 ml/min for the higher flow rates after a conditioning period of 24 h of flow perfusion culture. Media were changed three times per week with samples removed for analysis on days 4, 8, and 16.

In preliminary studies with this flow perfusion system, it was found that 1 ml/min (the medium flow rate in this study) was of sufficient stimulus to clearly alter the phenotypic behavior as compared to static culture. By then choosing to investigate half-log steps below and above (0.3 ml/min and 3 ml/min), we were able to investigate the effects of increasing fluid flow in the 3D perfusion culture of marrow stromal osteoblasts.

Static Culture. The seeded scaffolds were removed from the cassettes 1 d after seeding and cultured in standard 6-well culture plates with 10 ml of media following a media change schedule identical to that used for the flow perfusion culture systems. Samples for analysis were removed on days 4, 8, and 16 as well.

Analysis of Scaffold Cellularity. Cell/scaffold constructs were lysed by a freeze-thaw method in deionized distilled water (ddH_2O). The DNA content of the lysates was quantified by using a fluorometric DNA quantification kit (PicoGreen; Molecular Probes) with results expressed as cells per scaffold by quantifying the DNA content of a known amount of marrow stromal osteoblasts.

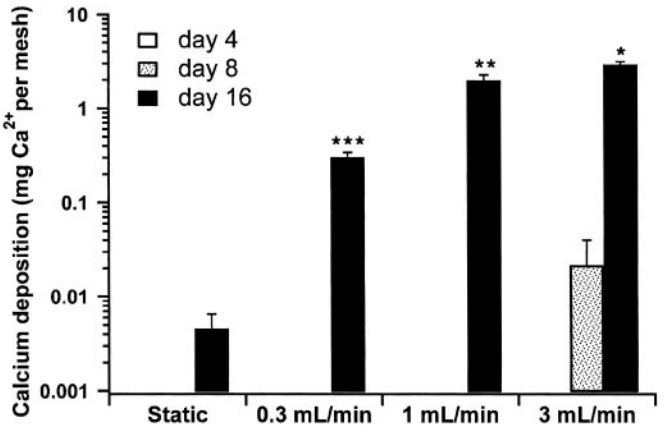

Fig. 2. Calcium content of cultured scaffolds. Results are expressed as mg Ca^{2+}/scaffold on a log scale. *, highest; **, second highest; and ***, third highest calcium content with each statistically different from all other groups ($P < 0.05$).

Alkaline Phosphatase (AP) Assay. Cell/scaffold constructs were lysed by a freeze-thaw method in ddH_2O. AP activity was determined by a colorimetric assay kit by using the conversion of *para*-nitrophenylphosphate to *para*-nitrophenol (kit 104-LL, Sigma).

Osteopontin Measurement. Osteopontin secreted in the culture media was measured by using a commercially available sandwich immunoassay specific for rat osteopontin (catalog no. 900-089), from Assay Designs (Ann Arbor, MI) The assay is based on two rabbit polyclonal Abs for rat osteopontin. One Ab is immobilized on a microtiter plate, and the second is labeled with the enzyme horseradish peroxidase.

Detection of Osteocalcin. Osteocalcin secreted in the culture media was measured by using a commercially available sandwich immunoassay (BT-490), specific for rat osteocalcin only, from BTI (Stoughton, MA) (31). The immunoassay is based on two goat osteocalcin Abs, recognizing both the carboxylated and the decarboxylated rat osteocalcin, each directed toward an end of the (C- or N-terminal) protein. The lowest detectable level of osteocalcin with this assay kit was 0.3 ng/ml.

Calcium Content. Scaffolds were incubated overnight in 0.5 M acetic acid to dissolve the calcium in the scaffolds. The calcium content of the solutions was then quantified by using a kit (procedure no. 587, Sigma), which uses the ortho-cresolphthalein complexone colorimetric method. Standards were prepared from a $CaCl_2$ solution and the results expressed as mg Ca^{2+} equivalents per scaffold. To ensure that calcium measurements accurately reflected active mineralization of the scaffolds by the cultured cells, unseeded titanium scaffolds were "cultured" under identical flow perfusion and static culture conditions for 16 d and no detectable calcium deposition occurred.

Scanning Electron Microscopy (SEM) Analysis. Samples were fixed in paraformaldehyde, dehydrated in a gradient series of ethanol, dried with tetramethylsilane, and sputter-coated with gold. Images were taken by using a JEOL G5000 scanning electron microscope.

Light Microscopy Analysis. Samples were fixed in formalin, dehydrated in a gradient series of ethanol, and embedded in glycol methacrylate (Technovit 7200 VLC, Exakt, Oklahoma City, OK). Thin sections (10 μm) were prepared by using the Exakt cutting and grinding system by using established techniques (32). Sections were stained with methylene blue/basic fuchsin and images were taken with a conventional light microscope equipped with a Canon digital image capture system.

Statistics. Results are expressed as means ± SD. Multiple pairwise comparisons were performed by using the Tukey-Kramer procedure at a significance level of 95%.

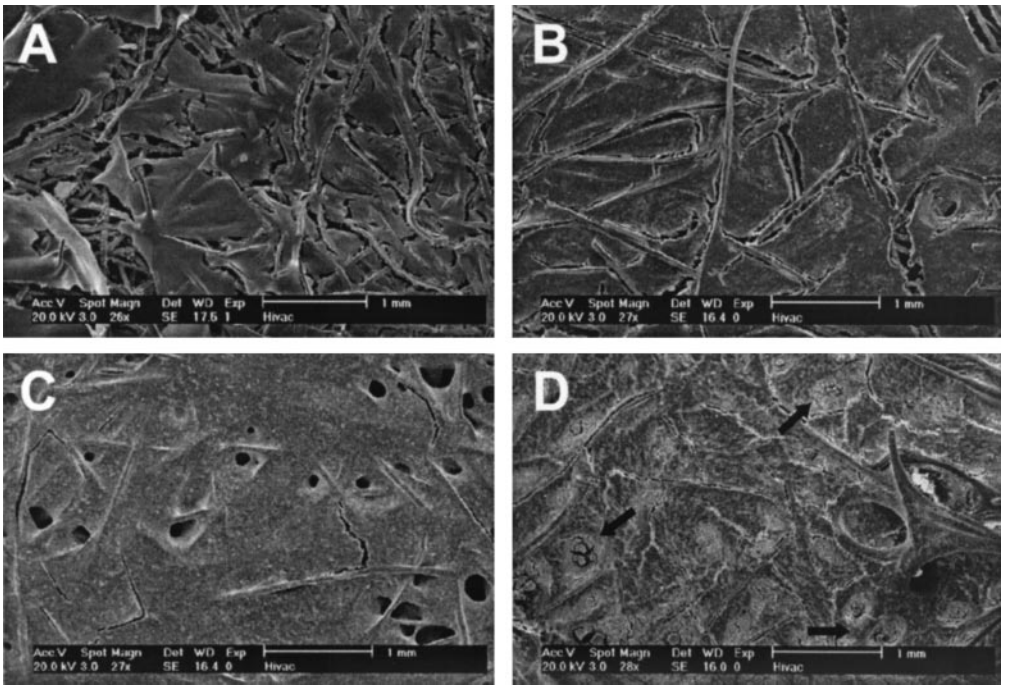

Fig. 3. SEM images of the surfaces of cultured scaffolds. Representative SEM images of surfaces of scaffolds cultured for 16 d with static culture (*A*), flow perfusion rate of 0.3 ml/min (*B*), flow perfusion rate of 1 ml/min (*C*), and flow perfusion rate of 3 ml/min (*D*). Porous structures formed during flow perfusion culture are readily apparent in *C*. Although less numerous, porous structures also were formed at the lowest perfusion rate. At the highest flow perfusion rate, the formed porous structures appeared to have become blocked or plugged with matrix. Several of these are indicated with arrows in *D*.

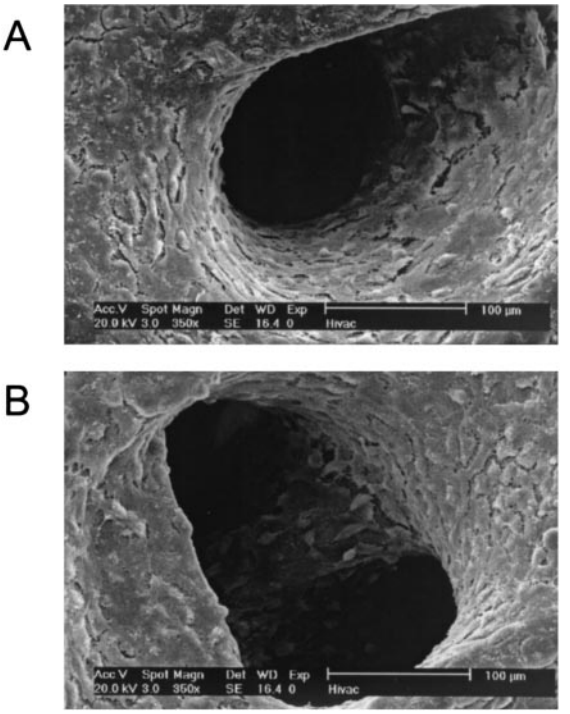

Fig. 4. Porous structures on surfaces of scaffolds cultured under flow perfusion. Higher magnification images of porous structures shown in Fig. 2*C*. Individual cells can be clearly seen lining the pores and deeper scaffold structures.

Results and Discussion

Flow Perfusion Culture of Marrow Stromal Osteoblasts. Marrow stromal osteoblasts were harvested from rat tibia, selected and expanded for 7 d in osteogenic media (29), seeded onto fiber mesh titanium scaffolds, and then cultured in a newly developed flow perfusion culture system for 16 d after seeding. This culture system permitted the study of differentiating marrow stromal osteoblasts as they proliferated and produced extracellular matrix in a 3D mechanically active environment. In addition, culturing seeded scaffolds at different flow rates of 0.3, 1, and 3 ml/min revealed dose-dependent effects of flow perfusion rate on mineralized matrix production, matrix modeling, and cell/matrix distribution.

Mineralized Matrix Deposition. By using a calcium dissolution assay, the amount of calcium contained in the scaffolds was quantified to evaluate the matrix production of the cultured marrow stromal osteoblasts. At all flow rates, the mineralized matrix contents of the scaffolds cultured for 16 d with flow perfusion culture were greatly increased over those cultured statically (Fig. 2).

Culturing seeded scaffolds with progressively higher flow rates in the flow perfusion system resulted in progressively higher levels of mineralization of the scaffolds (Fig. 2). A roughly 3-fold increase in flow rate from the lowest rate of 0.3 ml/min to the middle rate of 1 ml/min resulted in an over 6-fold increase in the calcium content of the cultured scaffolds. Increasing the flow rate further to the highest flow rate of 3 ml/min also resulted in an increase in matrix mineralization, but the magnitude of the increase was less, as a 3-fold increase in flow rate resulted in approximately twice as much calcium deposition. That the relationship between flow rate and mineral deposition was not linear throughout the range of flow rates suggests that there is a limit to the amount of matrix mineralization that can occur in this culture system.

The production of a mineralized matrix is considered the endpoint of full maturation of the osteoblast phenotype in differentiating marrow stromal cells, and flow perfusion culture at the higher rates appeared to have accelerated this differentiation (29). At the highest flow rate, marrow stromal cell-seeded scaffolds cultured under flow perfusion had already accumulated more calcium by day 8 than the statically cultured specimens had by the end of the culture period at day 16.

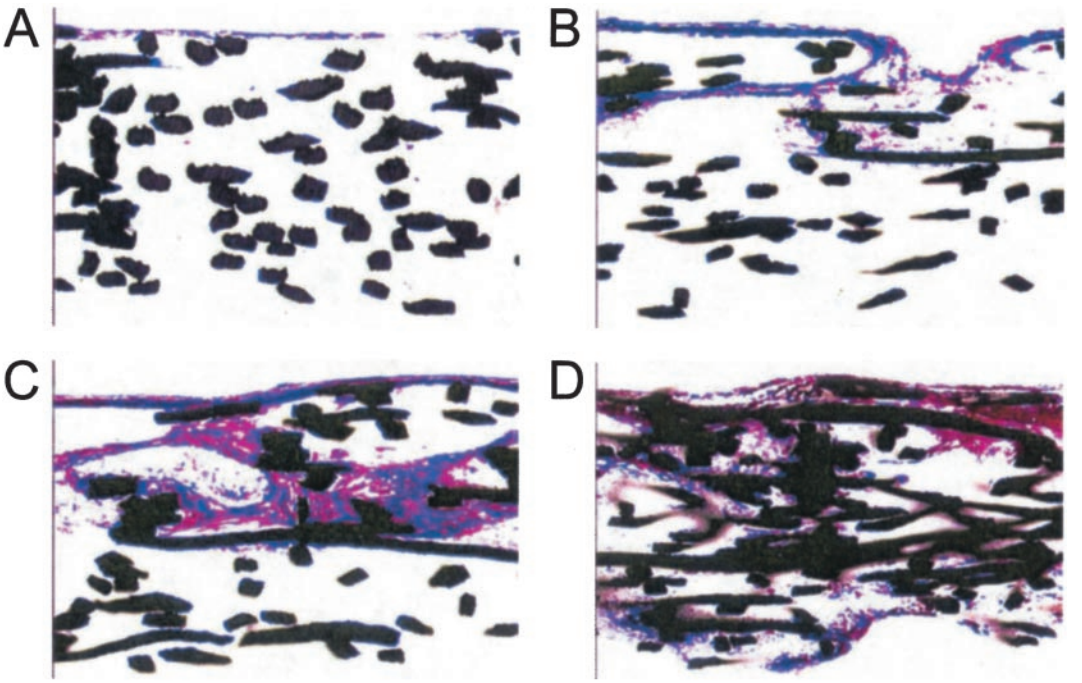

Fig. 5. Histological sections. Representative histological sections of scaffolds cultured for 16 d with static culture (*A*), flow perfusion rate of 0.3 ml/min (*B*), flow perfusion rate of 1 ml/min (*C*), and flow perfusion rate of 3 ml/min (*D*). Images are of histological crosssections of the cultured scaffolds. For flow perfusion culture specimens, the flow direction was from the top of the image through the scaffold to the bottom. Sections have been stained with basic fuchsin and methylene blue and viewed at ×10. The fibers of the titanium meshes appear black.

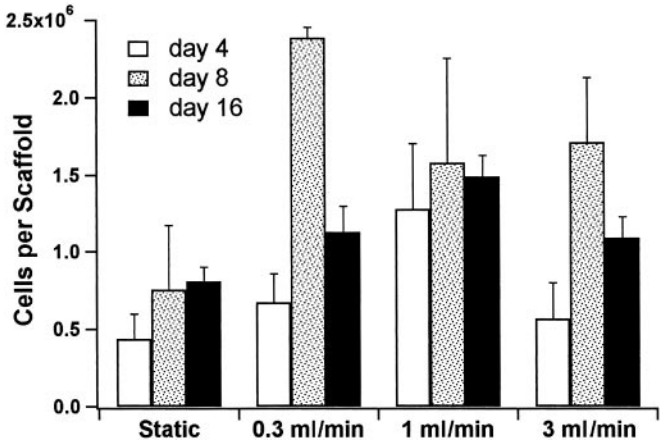

Fig. 6. Cellularity of cultured scaffolds. Results are expressed as cells per scaffold.

3D Matrix Modeling *In Vitro*. Examination of the cultured scaffolds at day 16 by SEM revealed that flow perfusion culture induced 3D modeling of the cultured cell/scaffold constructs (Fig. 3). Statically cultured specimens showed only a thin friable discontinuous crusting of extracellular matrix (Fig. 3*A*). Perfusion culture enhanced the matrix production even at the lowest flow rate whereas increasing the perfusion rate led to a thicker, more developed matrix (Fig. 3 *B–D*).

Discrete porous structures not seen with statically cultured specimens were observed on the surface in all perfusion-cultured samples at day 16. These porous structures were sparsely present on samples perfused at the low flow rate but were readily seen in abundance on the surface of the samples cultured at the medium and high flow rates (Fig. 3 *B–D*). However, it appeared that many of the porous structures had become obstructed or blocked because of overproduction of matrix at the highest flow rate (Fig. 3*D*). This may account for the previously mentioned nonlinear increase of mineralized matrix production with increasing flow rates.

Higher magnification examination of the porous structures revealed cells lining the surfaces of the porous structures and matrix on fibers deeper within the scaffolds (Fig. 4). The formation of these porous structures with organized cell growth and matrix arrangement suggests *de novo* tissue modeling because of the presence of penetrating fluid flow through the architecture of the underlying scaffold material.

Cell and Matrix Distribution. Histological sections revealed that flow perfusion culture dramatically improved the distribution of extracellular matrix through the cultured scaffolds (ref. 33; Fig. 5). Reinforcing what was seen with the SEM analysis, statically cultured specimens showed a thin crust of cells and matrix on the upper surface of the scaffolds where the marrow stromal osteoblasts were originally seeded (Fig. 5*A*). Again corroborating with what was shown in the SEM observations, even the low flow rate increased the amount and penetration of the developed matrix. With increasingly higher flow rates, the distribution of the matrix extended further throughout the scaffolds with the most uniform distributions obtained with culturing under the highest flow rate.

The cellularity of the titanium scaffolds was also measured on days 4, 8, and 16 of the culture period (Fig. 6). Although the histological data showed an effect of flow on the cell distribution, there was no clear trend with the cellularity of the scaffolds cultured under static culture or flow perfusion as determined by a fluorometric DNA assay. However, this may be caused by underestimation of DNA entrapped within the more mineralized tissue of the flow culture specimens.

Early Osteoblast Differentiation. As a marker of early osteoblastic differentiation (29), the AP activities of the constructs were measured on days 4, 8, and 16 of the culture period (Fig. 7). The typical rise and fall of AP activity characteristic of osteoblastic differentiation was common to all culture systems (29). However, at all time points the AP activity was significantly higher in the flow perfusion cultures when compared with static culture. There was although no apparent effect of varying flow rates on AP activity implying that the influences of higher flow perfusion rates predominantly affected the later osteoblastic differentiation, characterized by mineralization, more than the early osteoblastic differentiation, characterized by AP activity.

Late Osteoblast Differentiation. Osteopontin is a phosphorylated glycoprotein synthesized by osteoblasts that is associated with the early stages of osteogenesis preceding mineralization (34). It is hypothesized that osteopontin is secreted by osteoblasts at an early stage of bone development and promotes cell attachment necessary for mineralization of the matrix (35).

The osteopontin secreted into the culture media was measured at each media change and is presented in Fig. 8. Osteopontin was detected in all culture systems, although comparably lower peak levels were found in the scaffolds cultured under static conditions. With scaffolds cultured under flow conditions, there was a temporal pattern to the rise-and-fall expression of osteopontin (36) with peak levels occurring between days 5 and 8 for the high flow rate, between days 11 and 13 for the medium flow rate, and lastly

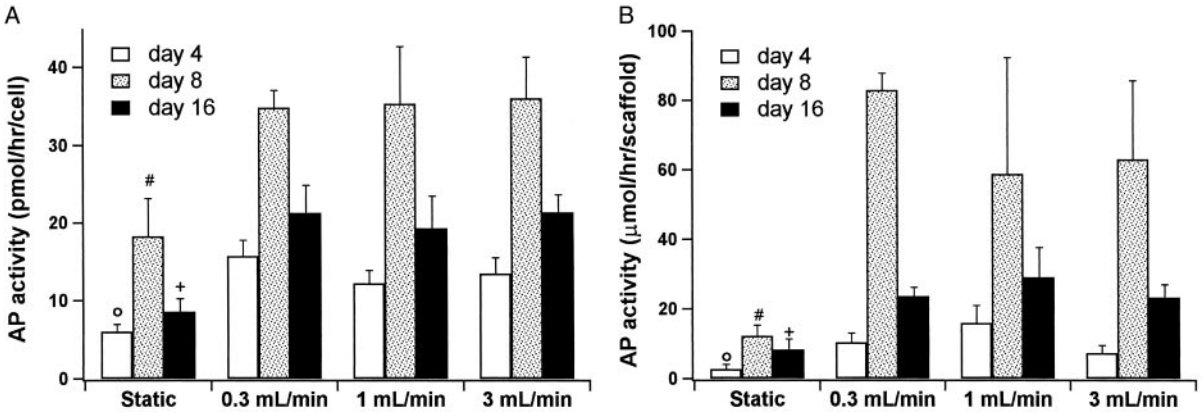

Fig. 7. AP activity of cells on cultured scaffolds. (*A*) Results are expressed as pmol/hr per cell. (*B*) Results are expressed as μmol/hr per scaffold. The symbols indicate that at day 4 (○), day 8 (#), and day 16 (+) the statically cultured cells had significantly less AP activity than all flow perfusion culture groups at the corresponding day of culture.

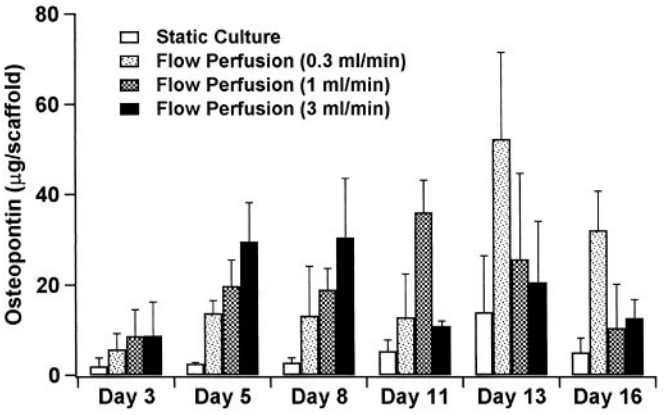

Fig. 8. Osteopontin secretion from cultured scaffolds. Results are expressed as microgram (μg) of osteopontin per scaffold.

between days 13 and 16 for the slow flow rate. This suggests an acceleration in the osteoblastic differentiation of the perfusion cultured cells that depends on fluid flow rate. This trend of accelerated osteoblastic differentiation seen with this early marker osteopontin is in accordance with the late marker of osteoblast differentiation, calcium deposition, with an earlier onset seen in flow perfusion cultures at the high flow rate (Fig. 1).

Osteocalcin, another marker of late-term osteoblast maturation (29, 36), was detected in the media of all culture systems from day 13 onward. This result suggests that, in all culture systems, the cells had differentiated into mature stromal osteoblasts.

Conclusions

Flow perfusion culture can exert its effects on osteoblasts through several different mechanisms including both fluid shear forces and enhancement of chemotransport. In this study, the initial shear forces experienced by the cells cultured on scaffolds under flow perfusion conditions did not exceed 1 dyne/cm^2 (1 dyne = 10 μN) as calculated by using a cylindrical-pore model approximation for the geometry of the scaffold porosity (24). This is at the lower limit of what previous studies have indicated is sufficient to induce stimulatory effects in bone cells (9, 13, 37–39). Although the stimulation of osteoblastic cells by fluid shear forces for a short period is well documented, the effect of continuous stimulation by fluid shear forces for an extended period on differentiating osteoblastic cells affecting their osteoblastic maturation and deposition of mineralized matrix has not been clearly elucidated. It may be that the impact of shear forces over a much greater time, weeks as opposed to hours, is significant even at these lower shear rates. The *de novo* tissue modeling occurring with the appearance of fluid flow-induced porous structures at even the lowest flow rate suggests that the osteoblasts are sensitive even to these limited mechanical influences.

Additionally, as the osteoblasts secrete extracellular matrix, a phenomenon that can only be observed in long-term fluid flow studies such as this one, the actual experienced shear rates dynamically increase with culture time as the matrix occupies an increasingly larger amount of the cultured scaffold. This increase in matrix decreases the porosity of the scaffolds, which can dramatically increase the shear forces experienced by the cells to values known to be stimulatory to osteoblastic cells in previous shorter-term studies (>2 dynes/cm^2). During the early portion of the culture period, there is a limited amount of mineralized matrix production and differences between specimens cultured under flow perfusion and static conditions reflect the enhanced nutrient transport found with perfusion culture. This is reflected in the data shown here, as fluid flow uniformly improved AP activity without apparent effect of flow rate as the shear stresses experienced by the cells were not sufficiently high. During the later culture periods, the osteoblasts continue to differentiate and deposit increasing amounts of mineralized matrix. The shear stresses experienced by these cells increase as the porosity of the scaffolds decreases. This restriction of the fluid flow path is readily apparent in the SEM and histological analysis. As would be anticipated for osteoblasts in a mechanically stressed environment, they respond to the increasing mechanical stimulation with increased production of mineralized matrix.

These studies performed with this newly developed flow perfusion system demonstrate the effects of increasing fluid flow on osteoblasts and the hallmarks of their phenotypic developmental pathway, mineralized matrix production, and 3D organization. A system that permits the generation and study of a 3D, actively modeled, mineralized matrix can be a valuable tool for both bone biology and tissue engineering.

This work was supported by National Institutes of Health Grant RO1-AR42639 and National Aeronautics and Space Administration Grant NAG5-4072. G.N.B. is supported by a Transco Energy Corporation MD/Ph.D. scholarship.

1. Buckwalter, J. A., Glimcher, M. J., Cooper, R. R. & Recker, R. (1995) *J. Bone Jt. Surg. Am. Vol.* **77,** 1256–1289.
2. Klein-Nulend, J., van der Plas, A., Semeins, C. M., Ajubi, N. E., Frangos, J. A., Nijweide, P. J. & Burger, E. H. (1995) *FASEB* **9,** 441–445.
3. Owan, I., Burr, D. B., Turner, C. H., Qiu, J., Tu, Y., Onyia, J. E. & Duncan, R. L. (1997) *Am. J. Phys.* **273,** C810–C815.
4. Smalt, R., Mitchell, F. T., Howard, R. L. & Chambers, T. J. (1997) *Am. J. Phys.* **273,** E751–E758.
5. Hung, C. T., Pollack, S. R., Reilly, T. M. & Brighton, C. T. (1995) *Clin. Orthop.* **313,** 256–269.
6. You, J., Reilly, G. C., Zhen, X., Yellowley, C. E., Chen, Q., Donahue, H. J. & Jacobs, C. R. (2001) *J. Biol. Chem.* **276,** 13365–13371.
7. Bakker, A. D., Soejima, K., Klein-Nulend, J. & Burger, E. H. (2001) *J. Biomech.* **34,** 671–677.
8. Ajubi, N. E., Klein-Nulend, J., Alblas, M. J., Burger, E. H. & Nijweide, P. J. (1999) *Am. J. Physiol.* **276,** E171–E178.
9. Johnson, D. L., McAllister, T. N. & Frangos, J. A. (1996) *Am. J. Physiol.* **271,** E205–E208.
10. You, J., Yellowley, C. E., Donahue, H. J., Zhang, Y., Chen, Q. & Jacobs, C. R. (2000) *J. Biomech. Eng.* **122,** 387–393.
11. Chen, N. X., Ryder, K. D., Pavalko, F. M., Turner, C. H., Burr, D. B., Qiu, J. & Duncan, R. L. (2000) *Am. J. Physiol.* **278,** C989–C997.
12. Pavalko, F. M., Chen, N. X., Turner, C. H., Burr, D. B., Atkinson, S., Hsieh, Y. F., Qiu, J. & Duncan, R. L. (1998) *Am. J. Physiol.* **275,** C1591–C1601.
13. Reich, K. M., Gay, C. V. & Frangos, J. A. (1990) *J. Cell. Physiol.* **143,** 100–104.
14. Kurokouchi, K., Jacobs, C. R. & Donahue, H. J. (2001) *J. Biol. Chem.* **276,** 13499–13504.
15. Reich, K. M., McCallister, T. N., Gudi, S. & Frangos, J. A. (1997) *Endocrinology* **138,** 1014–1018.
16. Piekarski, K. & Munro, M. (1977) *Nature (London)* **269,** 80–82.
17. Montgomery, R. J., Sutker, B. D., Bronk, J. T., Smith, S. R. & Kelly, P. J. (1988) *Microvasc. Res.* **35,** 295–307.
18. Otter, M. W., Bronk, J. T., Wu, D. D., Bieber, W. A., Kelly, P. J. & Cochran, G. V. B. (1996) *Clin. Orthop.* **324,** 283–291.
19. Burger, E. H. & Klein-Nulend, J. (1999) *FASEB* **13,** S101–S112.
20. Pienkowski, D. & Pollack, S. R. (1983) *J. Orthop. Res.* **1,** 30–41.
21. Pollack, S. R., Petrov, N., Brankov, G. & Blagoeva, R. (1984) *J. Biomech.* **17,** 627–636.
22. Jacobs, C. R., Yellowley, C. E., Davis, B. R., Zhou, Z., Cimbala, J. M. & Donahue, H. J. (1998) *J. Biomech.* **31,** 969–976.
23. Mueller, S. M., Mizuno, S., Gerstenfeld, L. C. & Glowacki, J. (1999) *J. Bone Miner. Res.* **14,** 2118–2126.
24. Goldstein, A. S., Juarez, T. M., Helmke, C. D., Gustin, M. C. & Mikos, A. G. (2001) *Biomaterials* **11,** 1279–1288.
25. Kale, S., Biermann, S., Edwards, C., Tarnowski, C., Morris, M. & Long, M. W. (2000) *Nat. Biotechnol.* **18,** 954–958.
26. Cukierman, E., Pankov, R., Stevens, D. R. & Yamada, K. M. (2001) *Science* **294,** 1708–1712.
27. Harter, L. V., Hruska, K. A. & Duncam, R. L. (1995) *Endocrinology* **136,** 528–535.
28. Wozniak, M., Fausto, A., Carron, C. P., Meyer, D. M. & Hruska, K. A. (2000) *J. Bone Miner. Res.* **15,** 1731–1745.
29. Lian, J. B. & Stein, G. S. (1992) *Crit. Rev. Oral Biol. Med.* **3,** 269–305.
30. Maniatopoulos, C., Sodek, J. & Melcher, A. H. (1988) *Cell Tissue Res.* **254,** 317–330.
31. Fante, P., Kindy, M. S., Mohaparta, S., Klein, J., Colombo, G. & Malluche, H. H. (1992) *Am. J. Physiol.* **263,** E1113–E1118.
32. Rohrer, M. D. & Shubert, C. C. (1992) *Oral Surg. Oral Med. Oral Pathol.* **74,** 73–78.
33. Vehof, J. W., de Ruijter, A. E., Spauwen, P. H. & Jansen, J. A. (2001) *Tissue Eng.* **7,** 373–383.
34. Mark, M. P., Butler, W. T., Prince, C. W., Finkelman, R. D. & Ruch, J.-V. (1988) *Differentiation (Berlin)* **37,** 123–136.
35. Butler, W. T. (1989) *Connect. Tissue Res.* **23,** 123–136.
36. Lian, J. B. & Stein, G. S. (1993) *J. Oral Implant.* **19,** 95–105.
37. Klein-Nulend, J., Burger, E. H., Semeins, C. M., Raisz, L. G. & Pilbeam, C. C. (1997) *J. Bone Miner. Res.* **12,** 45–51.
38. Hillsley, M. V. & Frangos, J. A. (1994) *Biotech. Bioeng.* **43,** 573–581.
39. Reich, K. M. & Frangos, J. A. (1991) *Am. J. Physiol.* **261,** C429–C432.